

Temperature dependence of Raman scattering in β -(AlGa)2O3 thin films

Xu Wang, Zhengwei Chen, Fabi Zhang, Katsuhiko Saito, Tooru Tanaka, Mitsuhiro Nishio, and Qixin Guo

Citation: *AIP Advances* **6**, 015111 (2016); doi: 10.1063/1.4940763

View online: <http://dx.doi.org/10.1063/1.4940763>

View Table of Contents: <http://scitation.aip.org/content/aip/journal/adva/6/1?ver=pdfcov>

Published by the [AIP Publishing](#)

Articles you may be interested in

[Simultaneous measurement of temperature and thermal stress in AlGaN/GaN high electron mobility transistors using Raman scattering spectroscopy](#)

J. Appl. Phys. **106**, 094509 (2009); 10.1063/1.3254197

[Temperature dependence of the E 2 h phonon mode of wurtzite GaN/AlN quantum dots](#)

J. Appl. Phys. **104**, 094904 (2008); 10.1063/1.3006892

[Far-infrared transmission in GaN, AlN, and AlGaN thin films grown by molecular beam epitaxy](#)

J. Appl. Phys. **104**, 033544 (2008); 10.1063/1.2968242

[Temperature dependence of the Raman-active modes in the nonpolar a -plane GaN film](#)

J. Appl. Phys. **101**, 023506 (2007); 10.1063/1.2424537

[Temperature dependence of the E 2 and A 1 \(LO \) phonons in GaN and AlN](#)

J. Appl. Phys. **86**, 6256 (1999); 10.1063/1.371681

An advertisement for AIP Applied Physics Reviews. It features a blue and orange background with a central image of a journal cover for "AIP Applied Physics Reviews". The journal cover shows a 3D schematic of a device structure. To the right of the journal image, the text "NEW Special Topic Sections" is displayed in large white letters. Below this, the text "NOW ONLINE" is in yellow, followed by "Lithium Niobate Properties and Applications: Reviews of Emerging Trends". At the bottom right, the "AIP | Applied Physics Reviews" logo is shown.

Temperature dependence of Raman scattering in β -(AlGa)₂O₃ thin films

Xu Wang, Zhengwei Chen, Fabi Zhang, Katsuhiko Saito, Tooru Tanaka,
Mitsuhiro Nishio, and Qixin Guo^a

*Department of Electrical and Electronic Engineering, Synchrotron Light Application Center,
Saga University, Saga 840-8502, Japan*

(Received 27 November 2015; accepted 11 January 2016; published online 22 January 2016)

We report a detailed investigation on temperature-dependent Raman scattering of β -(AlGa)₂O₃ thin films with different Al content (0-0.72) under the temperature range of 77-300 K. The temperature-dependent Raman shifts and linewidths of the phonon modes were obtained by employing Lorentz fitting. The linewidths broadening of phonon modes with the temperature can be well explained by a model involving the effects of thermal expansion, lattice-mismatch-induced strain, and decay of optical phonon into two and three phonons. It is clearly demonstrated dependence of the linewidths and decay process on the Al content in β -(AlGa)₂O₃ thin films, which can provide an experimental basis for realization of (AlGa)₂O₃-based optoelectronic device applications. © 2016 Author(s). All article content, except where otherwise noted, is licensed under a Creative Commons Attribution (CC BY) license (<http://creativecommons.org/licenses/by/4.0/>). [<http://dx.doi.org/10.1063/1.4940763>]

I. INTRODUCTION

Deep ultraviolet optoelectronic devices such as light detectors and emitters are paid more and more attention for their potential applications in biological and chemical agent detection, environmental protection, solar blind detection and high-density data storage.¹⁻⁴ As a wide variable bandgap semiconductor, ternary (AlGa)₂O₃ is a promising candidate for deep ultraviolet optoelectronic device applications because (AlGa)₂O₃ has an advantage of large tunable bandgaps from 4.8 eV (Ga₂O₃) to 8.6 eV (Al₂O₃) at room temperature.^{5,6} In order to realize (AlGa)₂O₃ application in deep ultraviolet optoelectronic devices, great efforts have made remarkable progress for growing this alloy.⁷ In our previous experiment, (AlGa)₂O₃ thin films were successfully deposited by pulsed laser deposition (PLD), and β -(AlGa)₂O₃ thin film could be obtained in the Al content range of 0-0.72.⁸ For further development of (AlGa)₂O₃-based optoelectronic device, detailed and reliable experimental data on the optical properties of β -(AlGa)₂O₃ thin films must be clearly investigated.

Compared with other spectroscopic techniques, Raman spectroscopy has a great of advantages such as nondestructive, no special sample preparation, and contactless.⁹⁻¹² Therefore, it has been widely employed in semiconductors. Kranert *et al.*¹³ have reported Raman spectra of (AlGa)₂O₃ films with different Al content (0-0.55) at room temperature. However, in contrast to the comprehensive investigation of temperature effect of Raman scattering for other semiconductors,^{14,15} temperature dependence of phonon behavior in β -(AlGa)₂O₃ thin films has not been reported up to now. The temperature dependent Raman linewidths and shifts can be interpreted in the terms of anharmonic processes which results in a better understanding of electronic properties of (AlGa)₂O₃ at different temperature.¹⁶ Moreover, it has been demonstrated that the anharmonic constant which was extracted by analyzing anharmonic processes is very important for the MgZnO-based light emission device applications.¹⁵ In this work, we reported on the temperature-dependence Raman scattering of β -(AlGa)₂O₃ thin films with different Al content (0-0.72) in the temperature range from 77 to 300 K. In combination with detailed theoretical modellings for the frequency downshift

^aCorresponding author. Tel +81 952 28 8662; fax: +81 952 28 8651. E-mail address:guoq@cc.saga-u.ac.jp (Qixin Guo)

and linewidths broadening, we can clearly illustrate the temperature effect on the Raman shift and linewidths in the β -(AlGa)₂O₃ thin films, which provides an experimental basis for realization of (AlGa)₂O₃-based optoelectronic device applications.

II. EXPERIMENT

The (AlGa)₂O₃ films used for present research were deposited by PLD using a KrF laser source ($\lambda = 248$ nm) on (0001) sapphire substrates. The (AlGa)₂O₃ bulks with Al content in the range of 0-0.72 were used as targets. The oxygen pressure during the growth was maintained at 1×10^{-1} Pa while the substrate temperature was kept at 400°C.⁸ The X-ray diffraction (XRD) revealed that the (-201), (-402), and (-603) diffraction peaks are observed from (AlGa)₂O₃ films together with the peak of (0006) reflection from sapphire substrate, indicating the patterns of monoclinic β -(AlGa)₂O₃.⁸ The atomic concentrations were estimated from X-ray photoelectron spectroscopy (XPS) element peak area by using an atomic sensitivity factor.⁸ The thickness of these (AlGa)₂O₃ films measured by using a surface step profile analyzer are between 200 and 300 nm. The surface morphologies and root mean square (RMS) roughness of (AlGa)₂O₃ films were characterized by atomic force microscope (AFM) as shown in figure 1.

The Raman spectra were recorded in the back-scattering geometry of the z (x, -) \bar{z} configuration¹⁷ by using a Horiba Jobin Yvon LabRAM HR 800 system equipped with an Andor DU420 classic charge-coupled device detector. The 488 nm line of Ar laser was used to excite the samples. The employment of a 50 \times optical microscopy objective with a numerical aperture of 0.5 will yield a laser spot size of ~ 0.8 μm . A Microstat^{HE} hot/cold stage (Oxford instruments) with a quartz window was used to heat the samples from 77 K to 300 K under flowing nitrogen. The temperature was controlled by a K-type thermocouple which has an accuracy of better than ± 1 K. For each measurement point, the temperature was kept for 10 min to avoid temperature fluctuations before acquiring a spectrum for 15 min. The power of the laser was set to about 2 mW to avoid thermal contributions coming from the laser.

III. RESULTS AND DISCUSSION

The monoclinic β -Ga₂O₃ belongs to the space group C2/m/C_{2h}³. The Raman-active modes of β -Ga₂O₃ can be classified into three groups: low-frequency libration and translation (below 200 cm^{-1}) of tetrahedra-octahedra chains, mid-frequency deformation of Ga₂O₆ octahedra (~ 310 -480 cm^{-1}), and high-frequency stretching and bending of GaO₄ tetrahedra (~ 500 -770 cm^{-1}).¹⁸ It has 27 optical phonon modes belonging to the irreducible representation

$$\Gamma^{\text{opt}} = 10A_g + 5B_g + 4A_u + 8B_u \quad (1)$$

Where symmetry A_g and B_g phonon modes are Raman active while phonon modes with A_u and B_u symmetry are infrared active.¹⁹

Figure 2 shows Raman spectra of (Al_xGa_{1-x})₂O₃ films with Al content x in the range of 0-0.72 measured at room temperature. For Ga₂O₃ film, six A_g and three B_g Raman active modes can be observed. The Raman peaks at 146.2, 169.6, 201.6, 351.3, 483.3, 656.4, and 767.4 cm^{-1} correspond to $B_g^{(2)}$, $A_g^{(2)}$, $A_g^{(3)}$, $A_g^{(5)}$, $A_g^{(7)}/B_g^{(4)}$, $A_g^{(9)}/B_g^{(5)}$, and $A_g^{(10)}$ phonon modes, respectively. The peak of $A_g^{(7)}/B_g^{(4)}$ phonon modes as well as $A_g^{(9)}/B_g^{(5)}$ can't be unambiguously assigned to one of the mode peaks $A_g^{(7)}$ or $B_g^{(4)}$ because Raman shifts of $A_g^{(7)}$ modes is very close to that of $B_g^{(4)}$ modes. The positions of these mode peaks have good agreements with those of Ga₂O₃ bulk and nanowires reported by other researchers.^{18,19} With the increase of Al content, the Raman active modes of (AlGa)₂O₃ films have a clear right shift. The Raman spectra also exhibit a line broadening for (AlGa)₂O₃ films at higher Al content. This broadening is particularly true for the Raman modes in mid-spectral range between 310 and 480 cm^{-1} , which is contributed to the more Al atoms entering into the crystal lattices of Ga₂O₃ to form ternary solid solution. For Al₂O₃ film, almost no peak can be observed except the Raman peak of sapphire substrates. Figure 3 shows the dependence of the spectral positions of $A_g^{(3)}$, $A_g^{(9)}/B_g^{(5)}$, and $A_g^{(10)}$ phonon modes on the Al content. As shown in

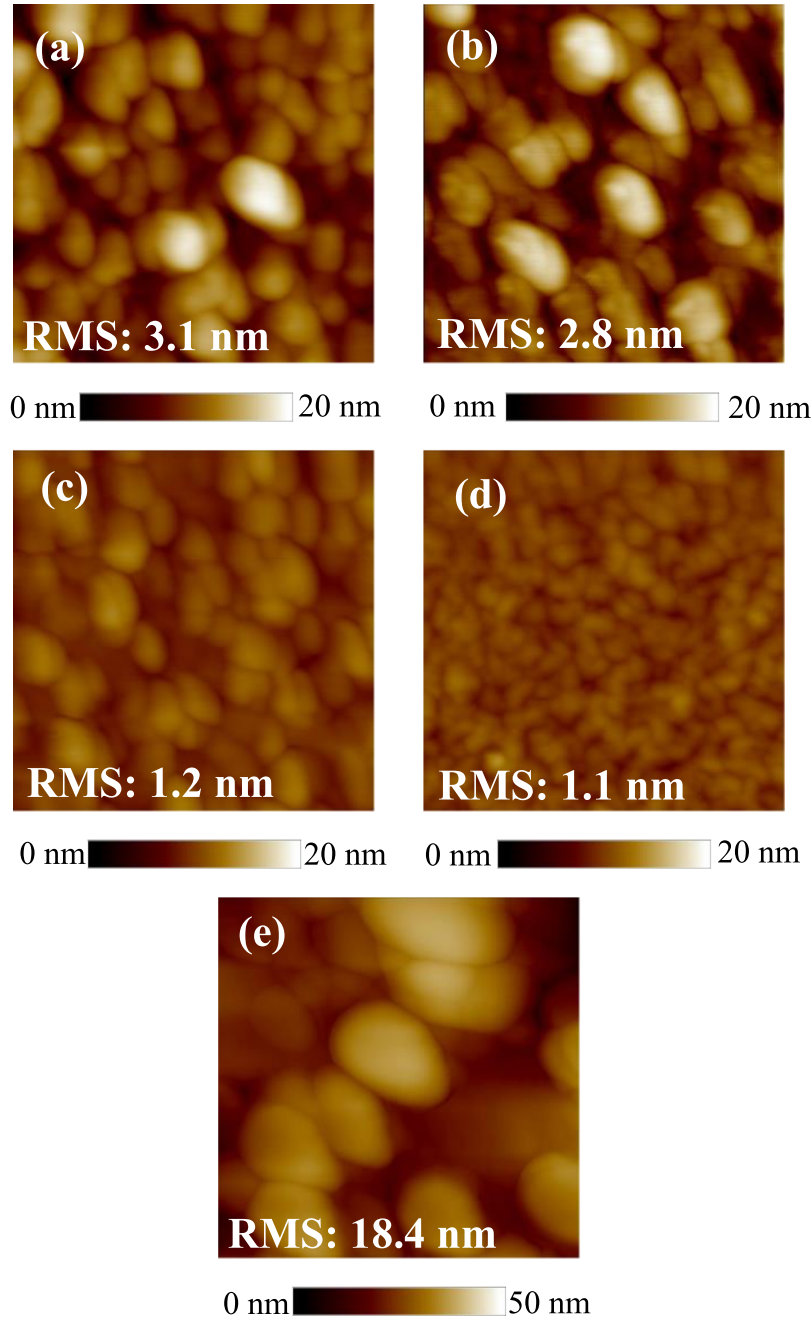


FIG. 1. AFM images of $(\text{Al}_x\text{Ga}_{1-x})_2\text{O}_3$ films with different Al content x of (a) 0, (b) 0.11, (c) 0.22, (d) 0.53, and (e) 0.72, respectively. The scan area is $1 \times 1 \mu\text{m}^2$.

figure 3, the Al content range of 0-0.72 the $A_g^{(3)}$ phonon mode exhibits a shift of $\sim 41 \text{ cm}^{-1}$, the $A_g^{(9)}/B_g^{(5)}$ phonon mode has a shift of $\sim 65 \text{ cm}^{-1}$, and the shift is $A_g^{(10)}$ phonon modes is $\sim 46 \text{ cm}^{-1}$.

Next, we measured the temperature-dependent Raman spectra of $(\text{AlGa})_2\text{O}_3$ films by keeping samples on the stage. Figure 4 presents the temperature-dependent Raman spectra of $(\text{AlGa})_2\text{O}_3$ films with Al content in the range of 0-0.72. The sharp Raman peaks of Ga_2O_3 films located at 201.6 and 767.4 cm^{-1} are attributed to the $A_g^{(3)}$ and $A_g^{(10)}$ phonon modes, respectively, while peaks at 418 , 520 , and 754 cm^{-1} are caused by sapphire substrate. Here, we note that in temperature-dependent Raman measurement process, some of Raman modes disappeared due to absorption of the window of the stage. These peaks can only be observed at lower temperature. In order to observe the

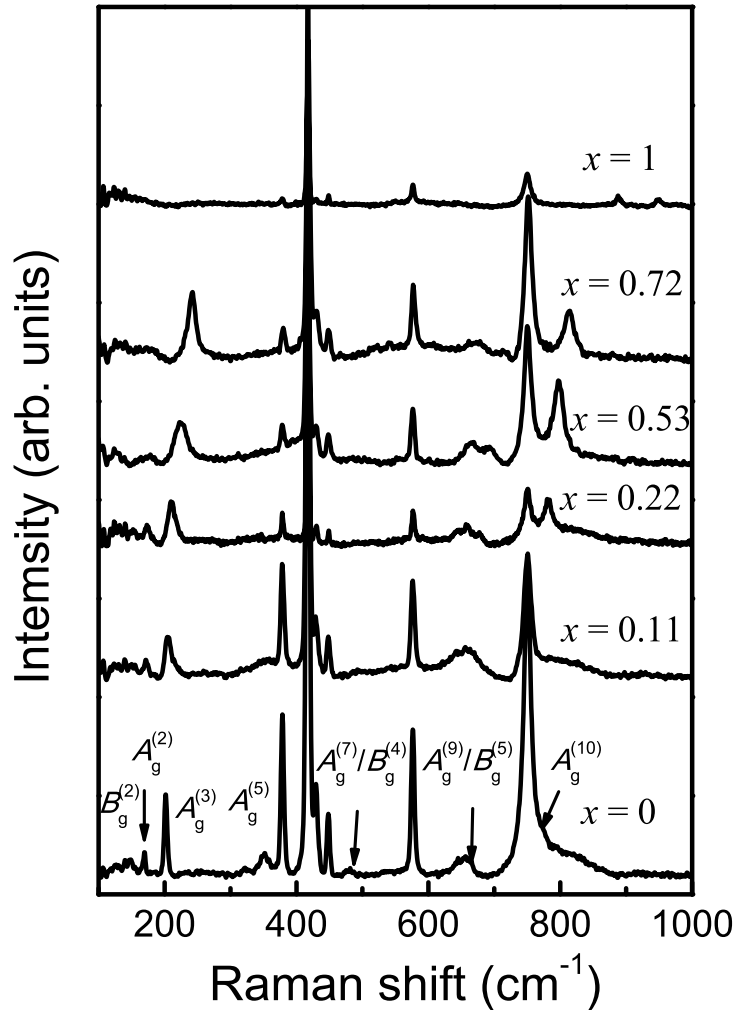


FIG. 2. Raman spectra of β -(AlGa)₂O₃ thin film with different Al content at room temperature.

temperature effect on the phonon modes in (AlGa)₂O₃ films, the enlarged Raman shift spectra of $A_g^{(3)}$ and $A_g^{(10)}$ phonon modes were shown in figure 5(a) and 5(b). The black solid curves are experimental Raman spectra. In order to obtain the more accurate information, a curve fitting program by using the Lorentz equation was employed to fit the experimental Raman spectra to determine the Raman shifts and linewidth broadening. The fitting curves are shown as red dash curves in figure 5(a) and 5(b). This approach has been shown to be very powerful for analyzing the contributions of different phonon modes in compound semiconductors such as AlInN and MgZnO.^{14,15}

Figure 6 shows the Raman shift of $A_g^{(3)}$ and $A_g^{(10)}$ phonon modes with temperature. It is clear that the $A_g^{(3)}$ and $A_g^{(10)}$ structure shifts to lower frequency with the increase of temperature. The temperature dependence of Raman shifts exhibit nonlinear behavior at the temperature from 77 to 300 K. In general, several factors are responsible for temperature-dependent Raman shift such as electron-phonon, anharmonic phonon-phonon interactions, and thermal expansion.^{20,21} However, for the effect of thermal expansion, the experimental structural information of (AlGa)₂O₃, such as Grüneisen parameters and phonon deformation potentials, was not established up to now. Therefore, There is no generally accurate method to describe the downshift of phonon frequencies in (AlGa)₂O₃ films with the increase of temperature at this moment.

Figure 7 shows the linewidths broadening of $A_g^{(3)}$ and $A_g^{(10)}$ phonon modes with temperature. It is clear that the linewidths broadening of $A_g^{(3)}$ and $A_g^{(10)}$ phonon modes increase with the increase of the temperature. With the increase of temperature, the thermal agitation increases, giving

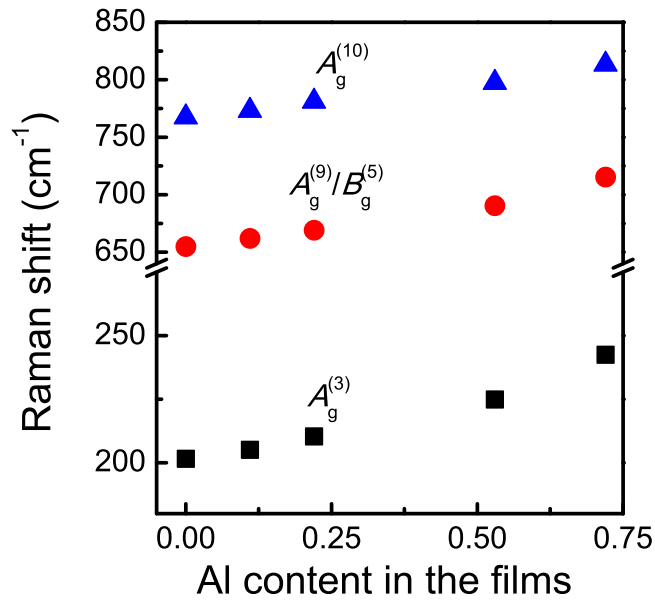


FIG. 3. Raman shifts of $A_g^{(3)}$, $A_g^{(9)}/B_g^{(5)}$, and $A_g^{(10)}$ phonon modes as a function of Al content.

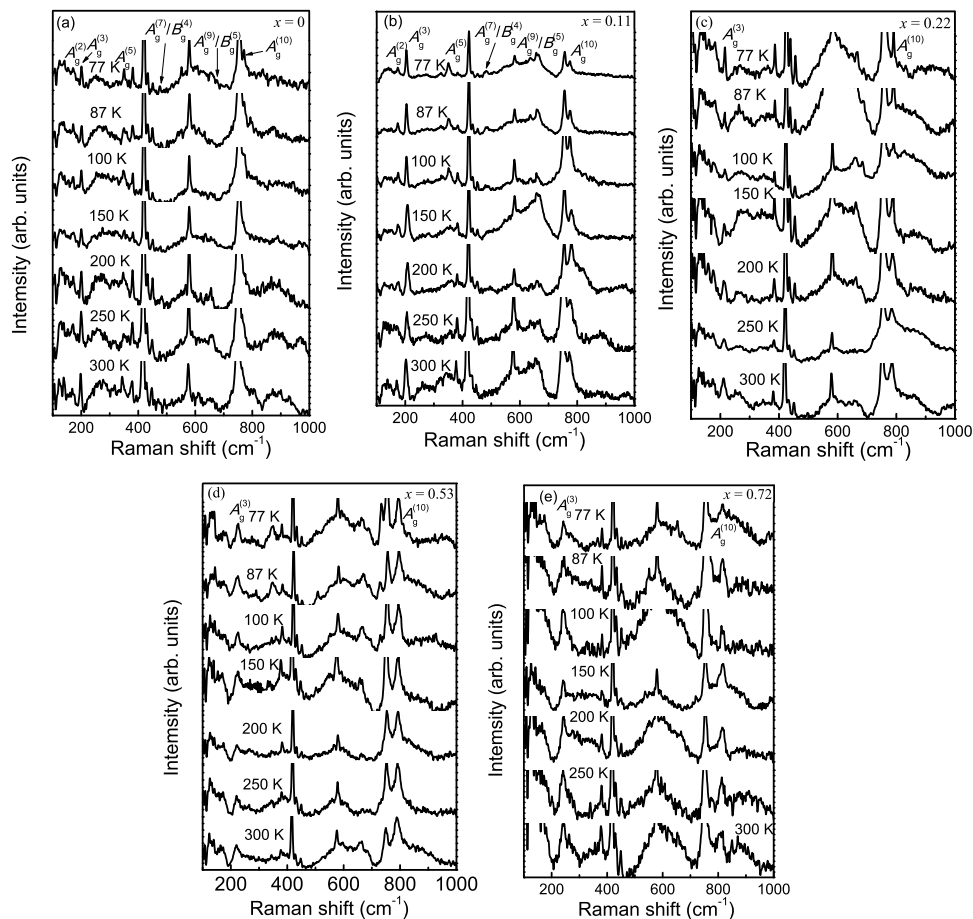


FIG. 4. Temperature dependence Raman spectra of β -(AlGa) $_2$ O $_3$ thin film with different Al content.

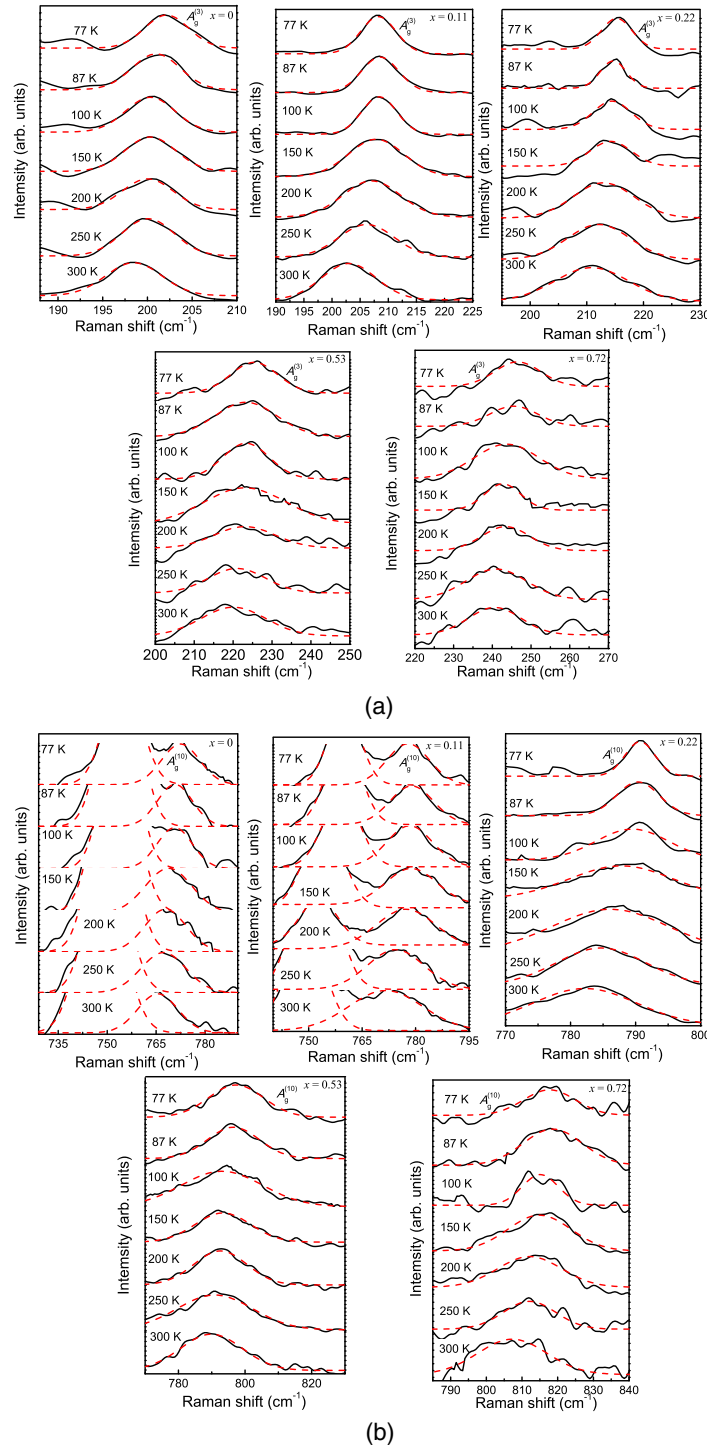


FIG. 5. Enlarge Raman spectra of (a) $A_g^{(3)}$ and (b) $A_g^{(10)}$ modes in β -(AlGa)₂O₃ thin film with different Al content.

rise to a decrease in the phonon mean free path, and so the decay lifetime (τ) decreases.²² The relation between decay lifetime and full width at half maximum (FWHM: Γ) can be written as $\tau = 1/(\pi c \Gamma)$, where c is velocity of light. Thus, FWHM increases with increasing temperature. Here, the approach developed by Guo *et al.*²³ was employed to explain linewidths broadening of $A_g^{(3)}$ and $A_g^{(10)}$ phonon modes. The temperature dependence of linewidths broadening is caused by

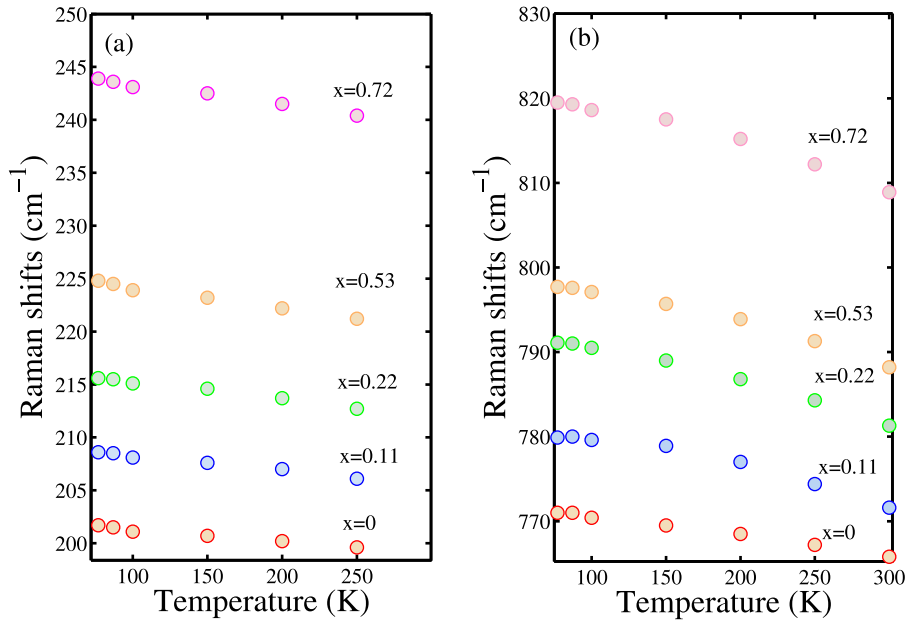


FIG. 6. Temperature dependence Raman shifts of (a) $A_g^{(3)}$ and (b) $A_g^{(10)}$ modes in β -(AlGa)₂O₃ thin film with different Al content.

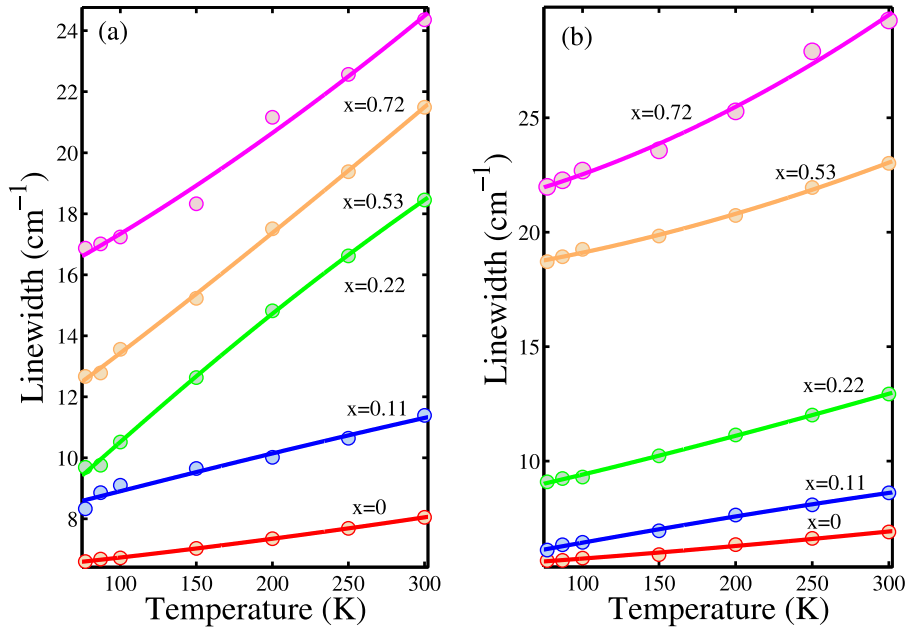


FIG. 7. Temperature dependence Raman linewidths of (a) $A_g^{(3)}$ and (b) $A_g^{(10)}$ modes in β -(AlGa)₂O₃ thin film with different Al content.

phenomenon of the optical phonon decay into two (three phonon process) or three (four phonon process) acoustic phonons with equal energies stemming from lattice potential cubic and quartic anharmonicity. The equation can be written as:

$$\begin{aligned}\Gamma(T) &= \Gamma_0 + \Gamma_1 + \Gamma_2 \\ \Gamma_1 &= A[1 + n(T, \omega_1) + n(T, \omega_2)] \\ \Gamma_2 &= B[1 + 3n(T, \omega_0/3) + 3n^2(T, \omega_0/3)]\end{aligned}\quad (2)$$

TABLE I. Fitting parameters for linewidth broadening of $A_g^{(3)}$ and (b) $A_g^{(10)}$ in β -(AlGa)₂O₃ thin film.

| Raman modes | x | Γ_0 | A | B |
|--------------|------|------------|--------|----------|
| $A_g^{(3)}$ | 0 | 6.169 | 0.1676 | 0.002631 |
| | 0.11 | 8.503 | 0.4655 | 0.002973 |
| | 0.22 | 9.515 | 1.396 | 0.09757 |
| | 0.53 | 12.57 | 0.8681 | 0.03628 |
| | 0.72 | 16.61 | 1.262 | 0.04589 |
| $A_g^{(10)}$ | 0 | 5.237 | 0.1481 | 0.00249 |
| | 0.11 | 6.079 | 0.4573 | 0.00344 |
| | 0.22 | 8.743 | 0.5135 | 0.004949 |
| | 0.53 | 17.87 | 0.6054 | 0.06737 |
| | 0.72 | 20.52 | 0.9693 | 0.09491 |

where Γ_0 is the linewidth at 0 K, and the fitting parameter A and B are anharmonic constants corresponding to the relative probability of the occurrence of each process. $n(T, \omega) = [\exp(\hbar\omega/k_B T) - 1]^{-1}$ is the Bose-Einstein function with \hbar Planck's constant divided by 2π and k_B Boltzmann constant. In equation (2), Γ_1 results from the decay of the zone-center phonons into two phonons considered as three phonon process, with $\omega_1 + \omega_2 = \omega_0$. In general, the simplest three phonon process for optical phonon decay, proposed by Klemens,²⁴ is decay into acoustic phonons of equal energy, $\omega_1 = \omega_2$, and opposite. And Γ_2 corresponds to the decay into three phonons (four phonon process), with the frequency $\omega_0/3$. ω_0 is the harmonic frequency of phonon mode. The solid curves shown in figure 7 are the fit of Eq. (2) for the temperature-dependent linewidths broadening of $A_g^{(3)}$ and $A_g^{(10)}$ phonon modes. The agreement between the theoretical fit and experimental data is very good. In addition, it is clear that the gradient of fitting curves increases with the increase of the Al content. Similar phenomena were also observed in AlInN and MgZnO alloy materials.^{14,15} The fitting parameters Γ_0 , A , and B have been obtained as shown in Table I. It is obvious that there is a rapid increase in Γ_0 with the increase of Al content because of the formation of lattice defect and structural disorder after Al implantation. Moreover, the dependence of Γ_0 on Al content play the closely related behavior with that of Urbach band tail according to report of Jiang, *et al.* In pure Ga₂O₃ film, Γ_0 of $A_g^{(3)}$ phonon mode is larger than that of $A_g^{(10)}$ phonon mode, implying that $A_g^{(3)}$ phonon mode is more strongly affected by impurity and/or defect scattering than that of $A_g^{(10)}$ phonon mode. However, Γ_0 of $A_g^{(10)}$ phonon mode increases much more rapidly with the increase of Al content than that of $A_g^{(3)}$ phonon mode. As we know, $A_g^{(10)}$ phonon mode belongs to high-frequency stretching and bending modes of GaO₄ tetrahedra.¹⁹ The stretching and bending modes involve the shortest Ga-O bonds (1.80 Å) which lead to more lattice defect and structural disorder when Al was implanted. These defects and disorders will result in strong enhancement of the impurity scattering in $A_g^{(10)}$ phonon mode of (AlGa)₂O₃ films.¹⁴ It is well known that the constants A and B can be related to the lifetime of the optical phonon decay into two (three phonon process) and three (four phonon process) acoustic phonons, respectively. It has been confirmed the inverse relation between the lifetime and the anharmonic constants.²² From Table I, it is obvious that the constants A and B increase with the increase of Al content. It can be explained that Al atom incorporation makes the more lattice defect and structural disorder which lead to shorten lifetime of decay process.

In order to better understand the contributions of the three phonon and four phonon processes in (AlGa)₂O₃ films, the ratios of A and B were calculated. Figure 8 displays the ratios of A and B for $A_g^{(3)}$ and $A_g^{(10)}$ phonon modes of Ga₂O₃ and (AlGa)₂O₃ films. It is obvious that the ratios of A and B are much larger than 1.0, indicating that the decay into two phonons is the prevailing process while the contribution from the four phonon processes is minor in the anharmonic coupling of $A_g^{(3)}$ and $A_g^{(10)}$ phonon modes. This result has a well agreement with the report on Ga₂O₃ bulk,¹⁸ which further indicates the reliability of our results estimated by theoretical fitting. For (AlGa)₂O₃ films, with the increasing of Al content, the ratios of A and B for $A_g^{(3)}$ and $A_g^{(10)}$ phonon modes decrease, indicating that the contribution from the three phonon process decreases after Al implantation. It can be explained by the increase of ω_0 in (AlGa)₂O₃ films leads to larger values of ω_1 and ω_2 , which

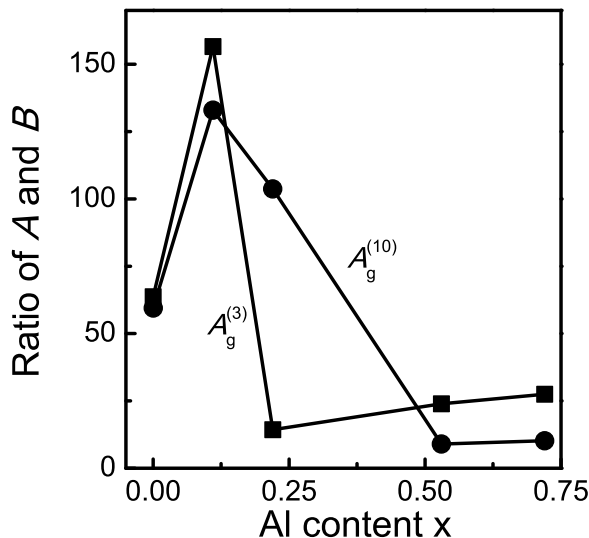


FIG. 8. Dependence of A/B on the Al content in β -(AlGa)₂O₃ thin films.

brings on the decrease of the contribution from the four phonon process.¹⁵ Moreover, it should be noted that three phonon process always dominates the linewidths broadening of $A_g^{(3)}$ and $A_g^{(10)}$ phonon modes in (AlGa)₂O₃ films.

The above results permit us to have a well understanding of the temperature effect on the Raman shift and linewidth in (AlGa)₂O₃ films, which establishes an experimental base for micro-Raman as a contactless, nondestructive, and fast method to monitor the local temperature during the operation of (AlGa)₂O₃-based devices with submicrometer spatial resolution.¹⁴ The obtained temperature and Al content dependence of Raman shift and linewidth can be used for deriving calibration curves as reported in MgZnO layer.²⁵ The local temperature for the (AlGa)₂O₃-based devices in operation can thus be determined by the calibration curve.¹⁴ Moreover, the information of the anharmonic effect is also important for the (AlGa)₂O₃-based device applications, because the degree of lattice disorder in mirrors by Raman microprobe spectroscopy correlates to the strength of facet heating and to the power limit at optical mirror damage.^{26,27}

IV. CONCLUSIONS

In this work, we investigated in detail the temperature-dependent Raman scattering of β -(AlGa)₂O₃ thin films in Al content range of 0-0.72 under the temperature range of 77-300 K. The temperature-dependent Raman shifts and linewidths of the $A_g^{(3)}$ and $A_g^{(10)}$ phonon modes were obtained by employing Lorentz fitting. Through the aid of a model involving the contributions of lattice-mismatch-induced strain, thermal expansion, and three and four phonon coupling, the effects of temperature on linewidths broadening were clearly illustrated. We demonstrated the dependence of the linewidths and decay process on the Al content in β -(AlGa)₂O₃ thin films. It is clearly observed that the three phonon process always dominates the linewidths broadening of $A_g^{(3)}$ and $A_g^{(10)}$ phonon modes in (AlGa)₂O₃ films. These results will provide an experimental basis for realization of (AlGa)₂O₃-based optoelectronic device applications.

ACKNOWLEDGEMENTS

This work was partially supported by the Partnership Project for Fundamental Technology Researches of Ministry of Education, Culture, Sports, Science and Technology, Japan.

¹ M. Khizar, Z. Y. Fan, K. H. Kim, J. Y. Lin, and H. X. Jiang, *Appl. Phys. Lett.* **86**, 173504 (2005).

² Z. Ren, Q. Sun, S. Y. Kwon, J. Han, K. Davitt, Y. K. Song, A. V. Nurmikko, H. K. Cho, W. Liu, J. A. Smart, and L. J. Schowalter, *J. Appl. Phys.* **91** 051116 (2007).

- ³ L. Wang, H. Xu, C. Zhang, X. Li, Y. Liu, X. Zhang, Y. Tao, Y. Huang, and D. Chen, *J. Alloys Compd.* **513**, 399 (2012).
- ⁴ L. Wang, J. Ma, H. Xu, C. Zhang, X. Ling, and Y. Liu, *Appl. Phys. Lett.* **102**, 031905 (2013).
- ⁵ H. Ito, K. Kaneko, and S. Fujita, *Jpn. J. Appl. Phys.* **51**, 100207 (2012).
- ⁶ R. S. Grund, C. Kranert, H. von Wenckstern, V. Zviagin, M. Lorenz, and M. Grundmann, *J. Appl. Phys.* **117**, 165307 (2015).
- ⁷ G. L. Li, F. B. Zhang, Y. T. Cui, H. Oji, J. Y. Son, and Q. X. Guo, *Appl. Phys. Lett.* **107**, 022109 (2015).
- ⁸ F. B. Zhang, K. Saito, T. Tanaka, M. Nishio, M. Arita, and Q. X. Guo, *Appl. Phys. Lett.* **105**, 162107 (2014).
- ⁹ J.R. Shealy and G. W. Wicks, *Appl. Phys. Lett.* **50**, 1173 (1987).
- ¹⁰ I. Calizo, A. A. Balandin, W. Bao, F. Miao, and C. N. R. Rao, *Nano Lett.* **7**, 2645 (2007).
- ¹¹ T. T. Kang, A. Hashimoto, and A. Yamamoto, *Phys. Rev. B* **79**, 033301 (2009).
- ¹² A.A. Balandin, *Nature Mater.* **10**, 569 (2011).
- ¹³ C. Kranert, M. Jenderka, J. Lenzner, M. Lorenz, H. V. Wenckstern, R. S. Grund, and M. Grundmann, *J. Appl. Phys.* **117**, 125703 (2015).
- ¹⁴ L. F. Jiang, J. F. Kong, W. Z. Shen, and Q. X. Guo, *J. Appl. Phys.* **109**, 113514 (2011).
- ¹⁵ J. F. Kong, W. Z. Shen, Y. W. Zhang, X. M. Li, and Q. X. Guo, *Solid State Commun.* **149**, 10 (2009).
- ¹⁶ M. S. Liu, L. A. Bursill, S. Prawer, and K. W. Nugent, *Appl. Phys. Lett.* **74**, 3125 (1999).
- ¹⁷ Q. X. Guo, M. Nada, Y. Ding, T. Tanaka, and M. Nishio, *J. Appl. Phys.* **107**, 123525 (2010).
- ¹⁸ R. Rao, A. M. Rao, B. Xu, J. Dong, S. Sharma, and M. K. Sunkara, *J. Appl. Phys.* **98**, 094312 (2005).
- ¹⁹ D. Dohy and J. Gavarri, *J. Solid State Chem.* **45**, 180 (1982).
- ²⁰ W. S. Li, Z. X. Shen, Z. C. Feng, and S. J. Chua, *J. Appl. Phys.* **87**, 3332 (2000).
- ²¹ X. D. Pu, J. Chen, W. Z. Shen, H. Ogawa, and Q. X. Guo, *J. Appl. Phys.* **98**, 033527 (2005).
- ²² P. Verma, S. C. Abbi, and K. P. Jain, *Phys. Rev. B* **51**, 16660 (1995).
- ²³ L. L. Guo, Y. H. Zhang, and W. Z. Shen, *Appl. Phys. Lett.* **89**, 161920 (2006).
- ²⁴ P. G. Klemecs, *Phys. Rev.* **148**, 845 (1966).
- ²⁵ A. Link, K. Bitzer, W. Limmer, R. Sauer, C. Kirchner, V. Schwegler, M. Kamp, D. G. Ebling, and K. W. Benz, *J. Appl. Phys.* **86**, 6256 (1999).
- ²⁶ P. W. Eppwelein, P. Buchmann, and A. Jakubowicz, *Appl. Phys. Lett.* **62**, 455 (1993).
- ²⁷ J. Jimenez, E. Martin, A. Torres, and J. P. Landesman, *Phys. Rev. B* **58**, 10463 (1998).